New Mexico Geological Society

Downloaded from: https://nmgs.nmt.edu/publications/guidebooks/76



Vesicle Cylinders in Vapor-Differentiated Basalt Flows, Revisited: Examples from New Mexico and Global Observations

Fraser Goff

2026, pp. 207-222. https://doi.org/10.56577/FFC-76.207

in:

Geology of the Albuquerque Region - Fall Field Conference 2026, Connell, Sean D.; Koning, Daniel J.;, New Mexico Geological Society 76th Annual Fall Field Conference Guidebook, 452 p. https://doi.org/10.56577/FFC-76

This is one of many related papers that were included in the 2026 NMGS Fall Field Conference Guidebook.

Annual NMGS Fall Field Conference Guidebooks

Every fall since 1950, the New Mexico Geological Society (NMGS) has held an annual Fall Field Conference that explores some region of New Mexico (or surrounding states). Always well attended, these conferences provide a guidebook to participants. Besides detailed road logs, the guidebooks contain many well written, edited, and peer-reviewed geoscience papers. These books have set the national standard for geologic guidebooks and are an essential geologic reference for anyone working in or around New Mexico.

Free Downloads

NMGS has decided to make peer-reviewed papers from our Fall Field Conference guidebooks available for free download. This is in keeping with our mission of promoting interest, research, and cooperation regarding geology in New Mexico. However, guidebook sales represent a significant proportion of our operating budget. Therefore, only *research papers* are available for download. *Road logs*, *mini-papers*, and other selected content are available only in print for recent guidebooks.

Copyright Information

Publications of the New Mexico Geological Society, printed and electronic, are protected by the copyright laws of the United States. No material from the NMGS website, or printed and electronic publications, may be reprinted or redistributed without NMGS permission. Contact us for permission to reprint portions of any of our publications.

One printed copy of any materials from the NMGS website or our print and electronic publications may be made for individual use without our permission. Teachers and students may make unlimited copies for educational use. Any other use of these materials requires explicit permission.

This page is intentionally left blank to maintain order of facing pages.

New Mexico Geological Society Guidebook, 76th Fall Field Conference, 2026, p. 207–221, https://doi.org/10.56577/FFC-76.207

VESICLE CYLINDERS IN VAPOR-DIFFERENTIATED BASALT FLOWS, REVISITED: EXAMPLES FROM NEW MEXICO AND GLOBAL OBSERVATIONS

FRASER GOFF[1]

[1]Department of Earth and Environmental Science, New Mexico Tech, 801 Leroy Place, Socorro, NM 87801; candf@swcp.com

Abstract—Vesicle cylinders (VC) are vertical pipes filled with bubbles and residual melt that differentiate from diktytaxitic pahoehoe basaltic flows during crystallization. They grow from about 0.25–0.5 m above the base of the flow to the bottom of the chilled flow top. Field relations limit their growth to the period between cessation of lava movement and deep penetration of columnar joints. An essential feature documented in VC and related vein-like structures called vesicle sheets (VS) is that they record the progressive chemical self-differentiation of basaltic host rock to residual glasses of trachyte–phonolite–rhyolite composition in single cylinders. Thus, their fractionation trends mimic those recorded in larger mafic bodies such as lava lakes, thick sills, and layered gabbros. Because VC and VS are more vesicular, coarse grained, and differentiated than their host lava, the basaltic magmas that favor their creation are considered to be relatively water rich, at least 0.4–0.5 wt% dissolved H_2O or perhaps considerably more. Understanding VC formation requires a comprehension of viscosity, density, cooling history, and other physical parameters inherent within basaltic lavas. For 6-m-thick flows of basaltic composition that cease movement, VC begin growth in as little as 1 day and cease growth in no more than 4 days. Thick pahoehoe flows such as flood basalts with complicated inflation and lava injection records have more complicated cooling relations. Most models describing VC formation conclude that they originate from density instabilities (such as Rayleigh–Taylor instability) developing at the bottom of cooling, water-rich flows. VC are identified in many basaltic flows in New Mexico and Arizona, but none of these flows have yet been studied in any detail. Field observations, thin sections, and chemical analyses of four New Mexico basalt–VC pairs presented herein show that they resemble those from other locations worldwide.

INTRODUCTION

I first studied the formation of vesicle cylinders (VC) and their fractionated contents in "vapor-differentiated" basalt flows nearly 50 years ago (Goff, 1977). This work, focused primarily on locations in the United States, was later refined in Goff (1996). Since then, many other researchers have investigated VC in a variety of host lavas from locations worldwide, and have documented their chemical differentiation, mineral composition, physical properties, and formation times and proposed a few new ideas about their growth mechanisms (e.g., Costa et al., 2006; Fowler et al., 2015). Yet some research issues and concepts regarding VC still need to be resolved, such as lateral continuity within flows, VC spacing and density, and sources of "excess" water. New Mexico contains nine sites with verified VC locations, mostly in basalts of olivine tholeiite composition (Table 1). Detailed study of VC at these sites could answer most of these lingering uncertainties.

BACKGROUND

Nomenclature—What's in a Name

Waters (1960, p. 357 and 359) illustrated field relations of vertical, vesicle-rich pipes extending from near the base of basalt lavas into their overlying lava cores. He called them "vesicle cylinders" (Figs. 1–3), and this terminology has since been used extensively in the United States (e.g., Bishop, 1969, fig. 2B; Gray, 1983, fig. 3). Kuno (1965) described several worldwide occurrences of fractionated (i.e., differentiated) material forming in situ within host lavas of basalt to andesite composition, which he termed "segregation veins." The Warner basalt in northeastern California also contains what he called "segregation cylinders," but he did not provide diagrams or photos of field relations. According to the *Glossary of Geology* (American Geological Institute, 2005), "magmatic segregation" is the concentration of crystals of a particular mineral (or minerals) in certain parts of a magma during its cooling and crystallization. The term is more or less synonymous with "igneous differentiation." Goff (1977, 1996) demonstrated that VC formed by "vapor-differentiation" and indicated that flows with VC also contained an overlying zone with "vesicle sheets" (VS; Figs. 1 and 2), which are equivalent to the segregation veins of Kuno (1965). Generally speaking, the rocks found within the cylinders, sheets, or veins are called segregations or differentiates. They are primarily products of fractional crystallization from the host basalt but generally contain some entrained groundmass of the host (Fig. 3A). As a result, numerous later research articles (mentioned below) now use the terms vesicle cylinders, segregation cylinders, etc., interchangeably.

Other names used for VC and associated VS are "pipe vesicles" (e.g., Hoffer, 1976, p. 16), "vesicle pipes" (Soderberg et al., 2024, fig. 9), "segregation structures" (e.g., Caroff et al., 2000), and "pegmatoid autoliths" (Rogan et al., 1996). The later term recognizes that VC and VS are coarser grained than their host lavas and contain products formed by in situ fractional crystallization, but this term is not widely used. Fowler

et al. (2015) proposed the nuanced name of "vesicular cylinders" for VC, but this term is not considered suitable because "vesicular" is so widely used to describe bubble-rich zones in mafic lavas of all types (Aubele et al., 1988; Cashman et al., 1994).

Terms such as "spiracles" (e.g., Waters, 1960), "pipe vesicles" (e.g., Philpotts and Lewis, 1987; Sheth, 2020), and "segregation vesicles" (Smith, 1967; Anderson et al., 1984; Merle et al., 2005) do *not* describe VC and VS, although in some cases pipe vesicles, which form at the very base of basaltic flows, can expand and develop VC above them. To avoid further confusion, the names "vesicle cylinders/sheets" or "segregation cylinders/veins" are used for the features described in this paper. The materials filling said VC and VS are called differentiates, fractionates, or magmatic segregations.

Where to Observe Vesicle Cylinders in Basaltic Flows

Exposed canyon walls and cliffs, highway and railway cuts, quarries, and eroded flow margins of *mafic pahoehoe lavas* are the best places to find VC (Fig. 2). Also, basaltic blocks that have fallen off cliff faces reveal both vertical and horizontal exposures of VC. Sea cliffs, sea benches, and exposed lakeshores are also good locations to observe physical relations (e.g., Rose and Olson, 2013), but prolonged exposure to water and sea spray degrades VC and VS for geochemical and mineralogical analysis. For example, the photos presented by Fowler et al. (2015, fig. 1) from the coast of Northern Ireland show VC as circular pits in horizontal exposures of massive lava because the frothy, differentiated, and once glass-rich cylinders erode and alter more quickly than the denser, more microcrystalline host rock.

VC and associated VS are visually distinct from host lavas and are sometimes used as decorative stone (Fig. 3A). In addition, metamorphosed VC and VS frequently contain various types of alterations and ore minerals that form colorful amygdules in once-open cavities (Figs. 3B and 3C).

TABLE 1. Locations of known basalt flows in New Mexico and Arizona with good examples of vesicle cylinders, sheets, and pods (Fig. 4).

Map no.	Name/site	Age (Ma)	Chem. type	Location (lat, long)*	Notes and references
New Mexico					
1	AV	0.199	OT	35.189, −106.686	Lower basalt flows, Albuquerque volcanic field, Petroglyph National Monument, Boca Negra and Piedras Marcadas Canyons (Goff, 1996; KellerLynn, 2017)
2	Cerro Verde	0.192	OT	34.797, −106.994	Cerro Verde basalt, Lucero volcanic field; upper cliff face above Rio San Jose in the South Garcia Quad (Goff, 1996; Maldonado et al., 2006)
3	Afton	>0.0429	AOB	31.972, −106.961	Afton basalt; upper flow unit(s) of lava exposed beneath maar deposits of Kilbourne Hole (Padovani and Reid, 1989; Goff, 1996; Zimmerer, 2024)
4	Ocate	0.81	OT	36.012, −104.710	Youngest lava of Ocate volcanic field; in road cut on NM 120 ~0.3 km west of I-25, Wagon Mound, New Mexico; has HTI in olivine (O'Neill, 1989)
5	Taos	3.3	OT	36.351, −105.737	Upper 2 flow units of Servilleta basalt exposed at top of west side of Rio Grande gorge on NM 267 (Thompson et al., 2017)
6	Taos	3.67	OT	36.476, −105.732	Upper flows of Servilleta basalt exposed north and south of west side of Rio Grande Gorge Bridge, US 64 (stop 4; Thompson et al., 2017, fig. 40)
7	Taos	≤3.5	OT	36.644, −105.956	Servilleta basalt west side of bridge across upper Rio Petaca, 1 km east of Tres Piedras, US 64; olivine has HTI (stop 17; Dungan et al., 1989)
8	Jemez Mountains	~9.0	HAT	35.786, −106.663	Paliza Canyon basalt; uppermost of four flows exposed in high cliffs of Church Canyon; olivine has HTI (F. Goff, unpublished data)
None	Zuni–Bandera	0.546	OT	34.726, −108.679	Flow top with fresh VS in road cut on NM 36; bottom of flow not exposed but may contain VC (Aoki and Kudo, 1976)
Arizona					
None	Springerville	3.67	OT	39.141, −109.209	Horseshoe Mountain basalt; flow 16 m thick overlies gravels on US 60, 5 km east of Springerville; has HTI (Laughlin et al., 1980, sample AWL-3-77)
None	Tucker Canyon	≤10	HAT	35.149, −112.660	Unnamed flow 10 m thick overlies Tapeats Sandstone, Yavapai County, Picacho Butte Quadrangle (Arney et al., 1985); part of Mt. Floyd volcanic field
None	Switzer Mesa	5.82	OT	35.196, −111.637	Basalt of Cedar Ranch; mesa top east side of Switzer Canyon near junction with old US 66, Flagstaff, AZ; olivine has HTI (Wolfe et al., 1987).

AOB = alkali olivine basalt; HAT = high-alumina tholeiite; HTI = high-temperature iddingsite (see text); OT = olivine tholeiite. *Decimal degrees; WGS 84 datum.

Key Physical Constraints and Variability

A diagram of the general field characteristics of VC and associated VS is shown in Figure 1 (Goff, 1977, 1996), which portrays relations for most pahoehoe flows 3–10 m thick. A stylized diagram of critical relations is also presented by Rogan et al. (1996). Several researchers have reported that VC and VS have greater average crystal size, coarser texture, greater vesicularity, darker color from increased contents of iron–titanium (Fe–Ti) oxides, and lower density than their host lava (e.g., Goff, 1977, 1996; Rogan et al., 1996). It is also worth noting that VS are relatively common in mafic lavas, whereas VC are comparatively rare.

Relatively slow effusion of pahoehoe flows (≤5–10 m^3/s; Roland and Walker, 1990) is key to the formation of VC because dissolved water can be better retained. High eruption rates (≥10 m^3/s) in broad a'a lava flows or channels do not favor VC formation, nor are VC found at scoria cones, fissures, dikes, etc. Lavas containing VC invariably have porous diktytaxitic textures (Fuller, 1931; Sakurai et al, 2024) that attest to the expansion of the intimate mixture of crystals and melt by water vapor during final stages of crystallization (e.g., Anderson et al., 1984, fig. 4; Rogan et al., 1996, p. 91; Hartley and Thordarson, 2009, fig. 4). VC usually occur at regularly spaced intervals (Goff, 1977, 1996), and their high vesicularity (porosity) causes differentiated liquids filling them to rise as low-density plumes or diapirs that feed an overlying network of VS near the flow top (Fig. 1). Cylinders generally begin growth within 0.25–0.5 m above the flow base but may begin at any higher level in the lower half of a flow. In continuous exposures, entire VC extend from locations near the base of the flow to the bottom of the chilled upper crust of the flow. VC trapped beneath the chilled upper crust form vesicle pods and/or splay into sill-like VS. VC vary from about 2 cm wide at flow bottoms to as much as 20 cm wide at their tops, and they increase in vesicularity upward. Higher in a flow, individual VC may merge to form broad collective cylinders. VC form after emplaced flows are virtually static. However, VC at certain horizons in a flow may be warped or bent in one direction, indicating some post-emplacement creep. Cooling joints form after VC are emplaced; consequently, many vertical exposures reveal VC as elliptical features.

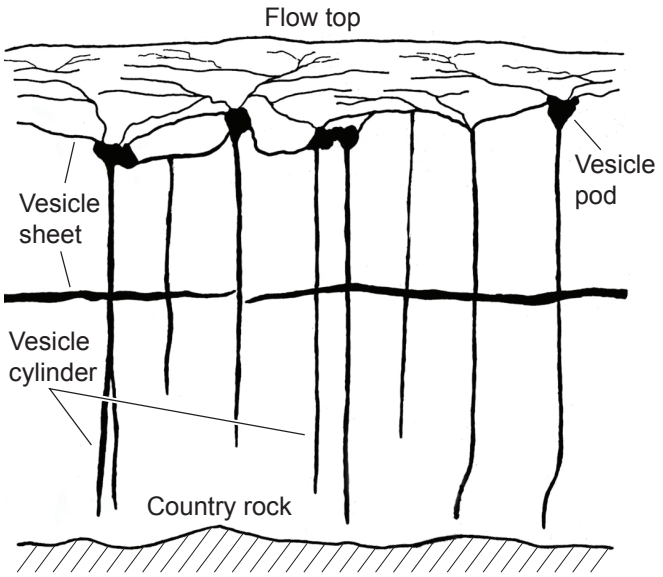


FIGURE 1. Idealized cross-section of basaltic lava (3–10 m thick) showing the network of vesicle cylinders, sheets, and pods. Warped cylinders near base of flow indicate that cylinders may form when the flow can still creep (modified from Goff, 1996).

On large horizontal surfaces in the lower half of a flow, VC generally show relatively uniform spacing. Such exposures reveal 30 or more VC/m^2, depending on the flow and the position of the exposure within the flow. Average closest spacing between VC can be <20 cm. The best sample locations to obtain VC and VS showing maximum fractionation are near the top of moderate- to large-diameter VC and near the upper horizon of thicker VS, to ensure that ensnared host rock fragments have settled out of rising differentiate. For more information on VC and associated VS characteristics and attributes in "typical" flows, consult Goff (1977, p. 8–32; 1996, p. 169–171) and photos and figures therein, or Rogan et al. (1996, p. 90–91).

Very thick, inflated pahoehoe flows such as "flood basalts" (e.g., Columbia River Basalt, CRB) can display disrupted, disturbed, and/or fragmented VC, implying that the initial formation of cylinders was partially destroyed by later injections of "isothermal" magma constantly passed through the flow (e.g., Hon et al., 1994; Thordarson and Self, 1996; Hartley and Thordarson, 2009, fig. 2). The upper crusts of flood basalt flows are generally thicker and more complicated than those in flows of "typical" thickness (e.g., 3–10 m). Otherwise, most of the features described above are essentially the same in thick flood basalt lavas.

In contrast to VC in lava flows of "typical" or much greater thickness, Sheth et al. (2017) described VC in pahoehoe flow lobes from a site in India that are a few meters long and a few decimeters thick. These VC erupted through the top of the flow lobe and have cylinder densities as large as 68/m^2 with a mean spacing of about 12 cm. The host lava has diktytaxitic texture, as in other VC-bearing flows, but no associated VS. The VC commonly form along prismatic joints and joint intersections. The fact that these pahoehoe lobes are so thin indicates that this lava cooled very rapidly, and the VC probably developed within a few minutes and no more than 1 hour after emplacement.

Finally, Merle et al. (2005) have described VC and VS in two hand-sized pillow lavas that were dredged from the Tore–Madeira Rise west of Portugal and from the Chile Triple Junction west of mainland Chile. Both samples have been altered by seawater interaction, but the former sample is borderline basanite, and the latter is basaltic andesite. Relations between VC, VS, and other "segregation structures" are somewhat different when compared between samples, but both pillows have diktytaxitic textures and both cooled rapidly in contact with seawater.

VESICLE-CYLINDER-BEARING FLOWS IN NEW MEXICO

I examined eight identified lava flows in New Mexico that contain VC and VS (Table 1; Fig. 2; Fig. 4, top). In addition, a Zuni–Bandera flow in western New Mexico contains an analyzed "coarse-grained segregation vein" in host basalt, which I recently examined (Aoki and Kudo, 1976; location in Table 1). All of these lavas erupted within the Rio Grande rift (RGR) or along the Jemez volcanic lineament (Goff and Kelley, 2020). None of the eight identified VC-bearing lavas have been researched in detail; thus, only four well-exposed examples are described below. Chemical analyses of well-located host and VC and VS pairs presented in Appendix 1 (four major-element pairs) and Appendix 2 (three trace-element pairs) provide the first comparative tabulation of precisely located flows from New Mexico. Also, three sites in Arizona that display outstanding VC and VS are listed on Table 1, although no detailed work has been published on them.

Albuquerque Volcanoes

The Albuquerque Volcanoes (AV; Table 1, Fig. 4, top) should be the best location for research and study of VC and VS in New Mexico. According to recent work (KellerLynn, 2017; Thompson et al., 2020; Zimmerer, 2024), the eruptions occurred

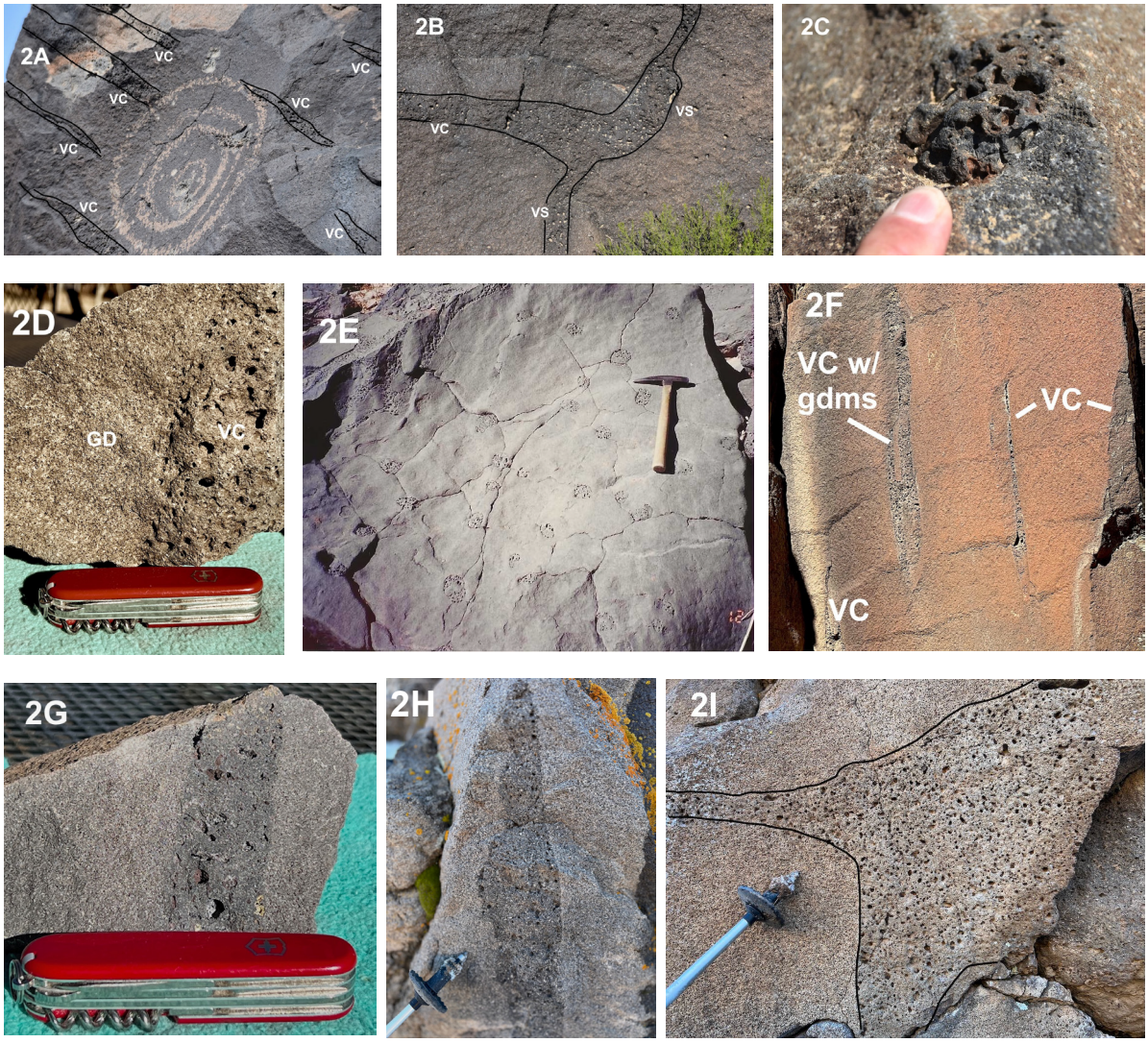


FIGURE 2. Selected photos of VC and associated VS features in New Mexico (photographed by F. Goff and C.J. Goff). A) Petroglyph carved into desert varnish on fallen block of AV basalt with seven VC (outlined in black). Determining the original "up" direction on isolated blocks can be challenging, but because cylinders expand upward, "up" was probably oriented ~25° toward the upper left. Photo taken from east path in Boca Negra Canyon. B) VC (horizontal, left) feeding a VS (undulating but near vertical) on fallen block in Boca Negra Canyon (outlined in black). The "up" direction is to the right. Note wind-blown sand/silt within large vesicles in VC and VS, and the pervasive desert varnish. C) Cross-section of VC in fallen block of AV basalt on Boca Negra Canyon trail. Because diameter is only ±2.5 cm, this cylinder is probably ±0.75 m above the base of the original undisturbed flow. Note coarse diktytaxitic texture of host lava and windblown sand/silt within larger vesicles. D) Photo of sample Goff-82 obtained from Piedras Marcadas Canyon during a field trip in 1982 (Appendix 1). Contact between groundmass (GD) and VC is quite sharp. Note coarse-grained diktytaxitic texture in GD and large bubble size within the VC. Diameter of VC is ~15 cm. E) Fallen basalt block in talus slope beneath Cerro Verde flow (site 2, Table 1) exposing at least 25 VC cross-sections with average spacing of 18 cm. Hammer handle is 30 cm long. F) Cliff face of Upper Servilleta Basalt (USB) along dirt road (site 5, Table 1) showing four VC, one with engulfed groundmass. G) Sample of VC in host lava from USB (site 5, Table 1 and Appendix 1). H) VC in coarse diktytaxitic USB, site 7, Table 1. I) Flaring VC (or vesicle pod) joining VS in USB, outlined in black (site 7, Table 1).



FIGURE 3. Examples of "unusual" VC. A) Two VC cross-sections in diktytaxitic basaltic curbstone along road beneath the Harbor Bridge, Sydney, Australia. Diameter of larger VC is ~10 cm. Note chunk of groundmass basalt engulfed within left VC. Source of basalt is unknown (photo by F. Goff and C.J. Goff). B) Cross-section of 10-cm-diameter VC filled with native copper, zeolite, and calcite in VC exposed along shore of Lake Superior in Precambrian Keweenaw Basalt, Isle Royale, Michigan (Rose and Olson, 2013). C) Cross-section of altered VC exposed in Keweenaw Basalt, Upper Peninsula, Michigan. Alteration: green = datolite, pink = adularia, white = zeolite/calcite. (Both photos F. Goff.)

at 199.5 ± 10.0 ka from several vents along a north-trending fissure system of the RGR that literally formed a large, east-thickening "puddle" of five to six flows covering an area of 62 km^2 (Baldridge, 1979; Connell, 2008).

The lavas are well exposed on the east due to erosion of underlying sediments near the Rio Grande, but they are partially covered to the west by younger sedimentary material. Consequently, VC are found in the lower two flows but have not been identified in upper flows.

However, several issues complicate research at this site. First, most of the good exposures of VC and VS are within the Petroglyph National Monument (PNM; KellerLynn, 2017); thus, observations are restricted to well-defined trails, with off-trail access normally forbidden. Second, sample collecting would be difficult given the multitude of spectacular petroglyphs protected by the PNM (Fig. 2A). Third, the basaltic flows and eroded blocks along cliffs and talus margins of the lower two flows are covered with a dark patina of desert varnish (Figs. 2A–2C). Although Baldridge (1979) recognized that AV flows contained VC, most geologists and volcanologists working there since then have not recognized their existence (L. Crumpler, personal communication, 2025). Fourth, Albuquerque and suburbs are expanding rapidly toward the east boundary of the PNM, preventing easy access on non-government lands. It's possible that blocks of VC-bearing basalt could be found in excavations within these new developments.

The AV flows are common olivine tholeiites (OT; Appendix 1; Baldridge, 1979). While on a field trip to AV led by Baldridge in 1982, I collected a sample of float from Piedras Marcadas Canyon (Fig. 2D). The VC of this sample is very distinct from the diktytaxitic host lava and shows four VC joining into a collective VC. The VC are coarser grained, more bubble-rich, and darker in color than the host basalt as a result of fractionation of residual liquids loaded with volatiles and Fe–Ti oxides that crystallized in the VC as it formed.

Appendix 1, which compares bulk rock major- and minor-element chemistry, shows that the VC differentiate in sample Goff-82 is chemically enriched in Ti, Fe, Mn, Ca, K, P, and Ba compared to the host lava. In contrast, Al, Mg, and Cr are depleted, and Si, Na, and Sr are about the same. Both host and VC contain carbon, but this probably reflects post-emplacement deposition of calcite (caliche) in the vesicular substrate.

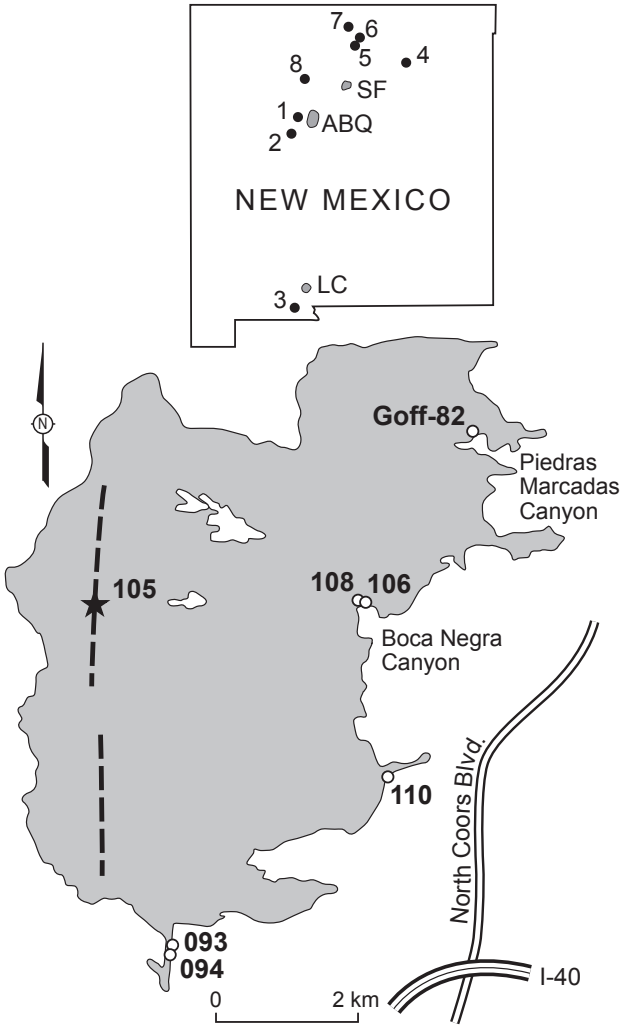


FIGURE 4. Location maps of New Mexico and Albuquerque Volcanoes (AV) area, respectively. Upper map of New Mexico shows numbered sites with located exposures of vesicle cylinders (Table 1 and Appendix 1). ABQ = Albuquerque; LC = Las Cruces; SF = Santa Fe. Lower map shows distribution of AV lava flows (dark gray), north-trending fissures along which eruptions occurred, a major eruption center (star), sample location Goff-82 in Piedras Marcadas Canyon, and locations of previously analyzed samples (modified from Baldridge, 1979).

Both host and VC contain ≤0.01 ppm sulfur. The major-element enrichments mimic fractional crystallization trends observed in basaltic to rhyolitic suites of rocks and mafic to felsic intrusive suites (e.g., Walker, 1956; Wager, 1960).

Trace-element chemistry data from analyses of Goff-82 host and VC are listed in Appendix 2. Most trace elements, including rare earth elements (REE), are enriched in the VC relative to host rock. Exceptions are Cr, Co, and Ni. Trace elements that do not show noticeable enrichment or depletion are Sr, Ge, Ta, and Mo.

Mineralogically, the chemical depletions and enrichments are easy to explain. Primary olivine phenocrysts contain chrome spinel inclusions and nickel in solid solution. Secondary olivine crystallized in the VC is progressively fayalitic—thus, relatively depleted in Mg, Cr, and Ni. Fe–Ti oxides in the VC differentiates are also depleted in Cr, Ni, and Co but are enriched in Mn. Calcic plagioclase is a primary mineral in the host basalt, whereas sodic plagioclase and potassium feldspar (K-feldspar) are progressively crystallized in the VC. This suggests upward flow of residual water-rich silicate liquid produced at the lower solidification front of the lava in the form of buoyant plumes.

Cerro Verde Basalt Flow

The Cerro Verde (CV) flow is roughly 20 km long and erupted 192.1 ± 5.1 ka (Maldonado et al., 2006; Zimmerer, 2024). It is part of the Lucero volcanic field on the west margin of the RGR. A beautiful cliff exposure occurs where US Highway 6 crosses the flow near its terminus (Table 1; Fig. 4, site 2). Large blocks of CV basalt with exceptional horizontal cross-sections are exposed as talus at the base of the flow (Fig. 2E; Goff, 1996). Average VC spacing is roughly 18 cm. VC density has not been accurately calculated, nor has the relation of VC to associated VS been studied. The host basalt is gray, medium-grained, and diktytaxitic, containing phenocrysts of olivine, plagioclase, augite, and Fe–Ti oxides in a groundmass of olivine, plagioclase, augite, Fe–Ti oxides, and glass. Cerro Verde VC are coarser grained and more vesicular than the host lava. They are apparently richer in Fe–Ti oxides and glass. Contrasting mineralogy has not been studied in detail.

CV basalt is common OT (Maldonado et al., 2006; Appendices 1 and 2). Chemical comparison of host rock and a single VC (collected in 1994) display the same enrichment and depletion trends in major-, minor-, and trace-element chemistry that are observed at the AV site. Possibly the chemical trends are more extreme than those in the AV example because the analyzed CV cylinder is relatively devoid of encapsulated host groundmass. The well-exposed CV basalt flow would be excellent for detailed study of VC and VS field relations and chemical variations, providing good information on terminal–proximal variations from the source vent.

Servilleta Basalt in Southern Taos Volcanic Field

Great exposures of VC and VS occur in the two uppermost lavas of Servilleta basalt along New Mexico Highway 267 as it crests the west margin of the Rio Grande gorge (Table 1, site 5; Figs. 2F and 2G; Thompson et al., 2017, p. 52). The upper flow has greater VC density. Both flows consist of gray, medium-grained diktytaxitic basalt containing phenocrysts of olivine, plagioclase, and augite. Average VC spacing and density have not been measured, nor has continuity been ascertained in exposures along the length of the canyon walls and across the gorge.

Basalt flows at this location are part of the Upper Servilleta Basalt (USB; e.g., Dungan et al., 1989) and are common OT (Appendices 1 and 2). These lavas apparently originated from the eroded vents of Tres Orejas northwest of the canyon. Chemical comparison of host and a single VC (collected in 2025) display the same enrichment and depletion trends in major-, minor-, and trace-element chemistry as are revealed at the AV site. Possibly the chemical trends are more extreme than those in the AV example because the analyzed USB cylinder was collected high in the outcrop and is devoid of encapsulated host groundmass.

Servilleta Basalt in West-Central Taos Volcanic Field

A fabulous exposure of VC with VS occurs on the southwest edge of an old bridge that crosses Rio Petaca below US Hwy 64 (Table 1, site 7; Figs. 2H and 2I). This USB outcrop is described by Dungan et al. (1989, stop 17). The source of the lava(s) is Cerro del Aire to the north. The lava consists of gray, exceptionally coarse-grained diktytaxitic USB with phenocrysts of olivine, plagioclase, and augite in a very frothy groundmass. Olivine phenocrysts display orange–red, high-temperature iddingsite alteration (Goff, 1996; Caroff et al., 2000). Average closest VC spacing is ≤25 cm; VC density has not been measured. The host lava consists of OT (Dungan et al., 1989, table 1), but analyses of the VC and VS have not been published. This is probably an ideal site for additional study of VC and VS because there are lengthy exposures of this unit along the Rio Petaca and neighboring ravines.

GEOCHEMISTRY OF HOST LAVAS AND THEIR VESICLE CYLINDERS/SHEETS

Variations in Host Lavas

Basic geochemistry of 45 VC-bearing host lavas from locations worldwide is shown in the total alkali versus silica (TAS) diagram of Figure 5 (Le Bas et al., 1986). The data in this plot provide a reasonably complete representation of host rock variations, which span compositions from borderline basanite to basaltic andesite. Most host rocks are basalt, and of these, most can be described as "common" OT. A subset of OT is high-alumina tholeiitic basalts (HAT) that contain ≥17 wt% Al_2O_3 (Kuno, 1960), although some workers prefer a cutoff of ≥16.5 wt% (e.g., Crawford et al., 1987). HAT are particularly common along volcanic arcs above descending slabs of subducted oceanic crust (Kuno, 1960). Some of the basalts plotted on this diagram were previously called alkali basalt (e.g., Togiak basalt AK, Hoare and Coonrad, 1980; and some lavas

of the Auckland, New Zealand, volcanic field, Rogan et al., 1996) because they have relatively high $Na_2O + K_2O$ and plot close to the boundary of alkalic and subalkalic magma compositions as earlier defined by Miyashiro (1978). VC-bearing host rocks that fall within the trachybasalt (also called hawaiite) field using the TAS diagram have not yet been identified or referenced. A possible exception is the VC-bearing flow of Afton basalt within Kilbourne Hole in southern New Mexico (Hoffer, 1976), which plots at the TAS boundaries of basanite–basalt–trachybasalt. Goff (1981) identified VC and VS in the CRB flows of both Sentinel Bluffs (e.g., Museum flow) and Wanapum Members (Priest Rapids, Roza and Frenchman Springs flows), but these lavas are basaltic andesite and basalt, respectively.

Host pahoehoe basalt flows commonly display little variation in chemistry top to bottom. For example, the ≤8-m-thick Crag Rat flow in Oregon has no significant chemical variation except in the ratio of Fe_2O_3 to FeO (eight analyses, normalized to 100%, loss on ignition (LOI) free; Goff, 1977, table 4 and p. 38). The 14–20-m-thick Levering flow (CRB) shows little chemical variability from top to bottom except in the basal crust zone (Hartley and Thordarson, 2009, fig. 6). However, the 7–8.5-m-thick Hafnarhraun flow (Iceland) shows some chemical variability attributed to multiple pulses of magma and/or gravitational settling of olivine in the core of the flow (Nikkola et al., 2019, p. 10).

Fractionation Trends in Vesicle Cylinders and Sheets

VC and associated VS contain chemically differentiated bulk-rock compositions reflecting fractionation of crystallized liquid from host lava. This can be seen by comparing analyses of host–VC/VS pairs (Appendices 1 and 2) or by examining fractionation trends of analyzed host, VC and VS, and basal/residual glasses on a total alkali–iron–magnesium (AFM) diagram (Fig. 6), a method applied by several authors (Goff, 1977, 1996; Merle et al., 2005; Hartley and Thordarson, 2009). AFM plots require bulk analyses of host and differentiate

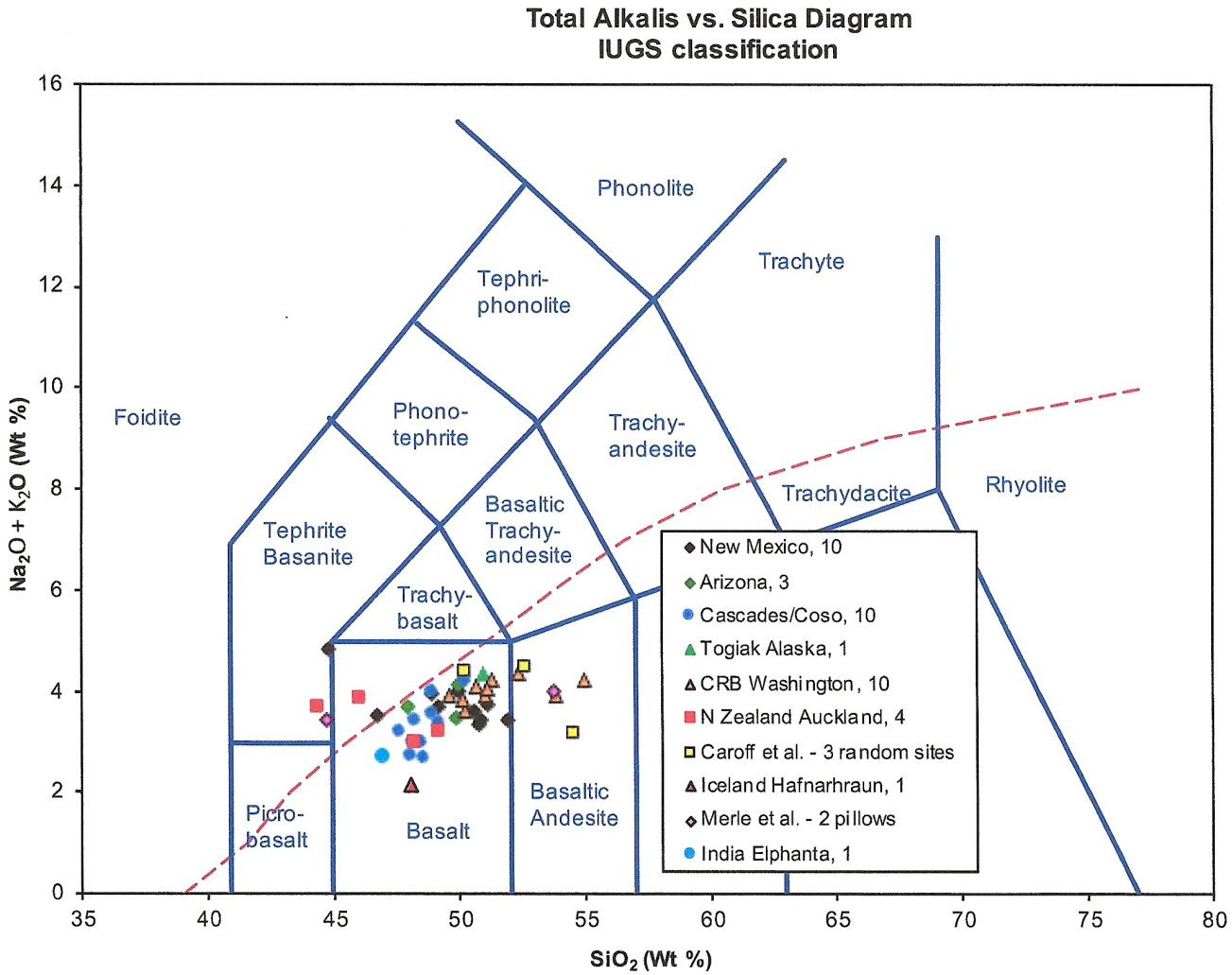


FIGURE 5. Total alkali vs. silica plot (Le Bas et al., 1986) showing compositions of 45 lavas that host VC and associated VS. All data from indicated locations are normalized to 100%, LOI free; numbers represent number of analyses used. Compositions identified range from borderline basanite to basaltic andesite. The majority of documented VC-hosted mafic rocks are subalkalic (calc-alkaline) according to red dashed boundary devised by Miyashiro (1978). None of the host rocks are trachybasalt to basaltic trachyandesite on a TAS plot. New Mexico data include analyses from all sites in Table 1 plus one analysis by Dungan et al. (1986) for which no location was provided. See text for discussion of data from other sites, which are available as Appendix 3.

pairs but also extensive analyses of glasses using an electron microprobe; thus, most reports on VC do not incorporate such diagrams in their discussions (e.g., Rogan et al., 1996; Caroff et al., 2000). However, AFM diagrams are useful for comparing fractionation trends in VC-bearing lavas to similar trends in lava lakes, layered gabbros, differentiated sills, etc. (e.g., Goff, 1977; Goff, 1996, fig. 7; Hartley and Thordarson, 2009, fig. 9).

Fractionation trends in VC-bearing lavas are also displayed on a TAS plot of all host–differentiate–glass compositions from separate flows (Fig. 7; see also Caroff et al., 2000, fig. 7). Host–VC/VS pairs from New Mexico show a "calc-alkaline" trend, but no residual glass analyses have been reported, and thus the trends are incomplete. The Levering flow (CRB), in which the host rock is basaltic andesite, also has a calc-alkaline trend. However, the dominant fractionation trend displayed by most representatives on this plot is "alkalic" from basalt to trachyte/trachydacite and even to rhyolite. The data from Auckland represent three bulk rock analyses from host and two differentiates in a single flow, and the trend there is also alkalic (Rogan et al., 1996). Admittedly, the residual glass data obtained by microprobe are scattered because the analyses are mostly of tiny patches of glass within the differentiates. Nonetheless, the trends represent fractionation trends.

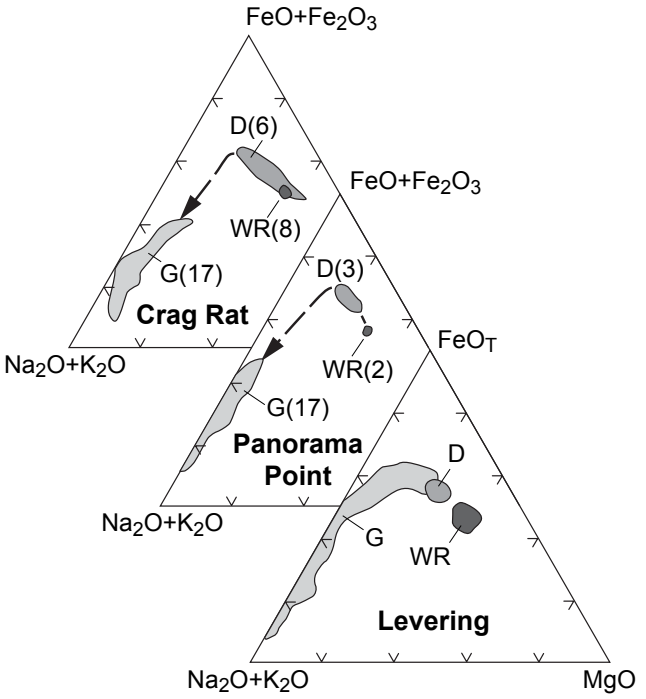


FIGURE 6. Total alkali-iron-magnesium (AFM) plots for three basaltic locations hosting VC and associated VS. Classic fractionation trends from basaltic to silicic end members are displayed in all cases. Data for each location include whole rock host (WR), VC and VS differentiate (D) analyses, and microprobe analyses of chilled basal crust glasses of host and residual glasses in VC and VS (G). Crag Rat and Panorama Point analyses are from HAT basalts, whereas Levering data are from CRB flood basalt. Plots are modified from Goff (1977, 1996) and Hartley and Thordarson (2009).

Fractionation of Trace and Rare Earth Elements

As mentioned above, differentiates in New Mexico VC are consistently enriched in most incompatible major and trace elements compared to their host lavas (Appendices 1 and 2; see also Goff, 1996, table 4; Rogan et al., 1996, fig. 3). Depleted (compatible) elements are usually Al, Mg, Cr, Ni, and Co, although there are variations depending on the samples and their contents of engulfed groundmass (Fig. 3A; see also Goff, 1996, fig. 5). Incompatible trace elements Ba, Rb, Zr, Nb, V, Zn, Th, U, and Y are always enriched in VC relative to host, usually by factors of 1.5–3; trace element Sc is barely enriched. REE, including Eu, in New Mexico VC are invariably enriched compared to host, usually by a factor of 1.5–2. Similar enrichments, but in smaller numbers of analyzed elements and/or samples, are reported by Rogan et al. (1996), Caroff et al. (2000), Merle et al. (2005), Hartley and Thordarson (2009), and Nikkola et al. (2019). Thus, in situ chemical fractionation recorded in host–VC/VS pairs mimics what is recorded in other types of igneous differentiation.

MINERALOGY OF HOST LAVAS AND VESICLE CYLINDERS/SHEETS

Host Lavas

Worldwide, all lavas hosting VC and VS are basaltic and display diktytaxitic texture. Bulk mineralogy of host lavas consists of the usual olivine, plagioclase, augite, Fe–Ti oxides, and glass, but proportions and compositions vary (e.g., Goff, 1977; Goff, 1996, table 3; Rogan et al., 1996, table 2). Some flows show ophitic to subophitic groundmass augite in thin section. OT and HAT lavas generally have phenocrysts of calcic plagioclase ($An_{82–60}$) and olivine ($Fo_{90–70}$) containing inclusions of magnesium-rich chromite. Fe–Ti oxides in HAT lavas (Goff, 1996) contain about 80% ulvospinel in magnetite and 5% R_2O_3 in ilmenite. The more alkaline lavas from Auckland contain phenocrystic augite and groundmass nepheline (Rogan et al., 1996). Hoffer (1976) reports minor feldspathoids (analcime?) in some Afton lavas (Table 1). The Levering basaltic andesite (CRB; Hartley and Thordarson, 2009) is rather aphyric and contains no olivine. Pillow lavas studied by Merle et al. (2005) contain phenocrysts and groundmass olivine, plagioclase, and glass, but no clinopyroxene.

Many flows hosting VC and VS contain olivine phenocrysts that display reddish-orange, high-temperature iddingsite (HTI) alteration around phenocryst margins and cracks, and some flows contain olivine with 50–100% HTI alteration (Goff, 1977; Goff, 1996, fig. 6b; Caroff et al., 2000, fig. 1c). The HTI alteration predates eruption of the lava because fresh overgrowths of fayalitic olivine ± augite partially cover the phenocrysts. Highly altered phenocrysts from the Panorama Point flow in Oregon were studied in Goff (1977, 1996) using X-ray diffraction and electron microscope techniques. The HTI was determined to be an intimate mixture of orthopyroxene, gamma-Fe_2O_3, alpha-Fe_2O_3, cristobalite, amorphous silica, and $Fe_2O_3 \cdot H_2O$. Because these hematitic phases coexist with magnetite, this mineral

assemblage indicates high oxygen fugacity in the magma at eruption, e.g., $\log_{10} fO_2$ of −3 to −4 at 1200–1150 °C along the hematite–magnetite buffer curve (e.g., Carmichael and Ghiorso, 1990; for practical application, see https://fo2.rses.anu.edu.au/fo2app/#:~:text=Resolution&text=Resolution).

Vesicle Cylinders and Sheets

VC and VS are more vesicular, coarser grained, and darker in color than their host lavas because they siphon fractionated gases (primarily water vapor) from host lava that create more vesicles and promote the growth of larger crystals. As this process continues, VC and VS concentrate fractionated iron, titanium, manganese, etc. that crystallize black Fe–Ti oxides. Focusing on minerals that distinguish maximum differentiation is the best way to contrast host lava and VC and VS. Goff (1977; 1996, table 3) showed that VC and VS in HAT contain fayalite (Fo_{25-8}), plagioclase (An_{35-50}), alkali feldspar (Or_{46-5}), iron-rich pyroxene, and in some cases aegirine (≤29 wt% FeO_T and ≤10 wt% Na_2O). Fe–Ti oxides were 62–79% ulvospinel and 4–10% R_2O_3. The alkali feldspar and aegirine result from extreme fractionation of potassium, sodium, and iron into the last crystallizing residues of VC and VS. Kuno (1965) also documented aegirine in VC and VS from the Warner (HAT) basalt, and Sigmarsson et al. (2005) identified aegirine–augite, as well as trace amphibole and nepheline, in VC and VS from Surtsey lavas (Iceland). The more alkaline basalts and basanites of Auckland possess differentiates that contain fayalite (up to Fo_{25}), plagioclase (up to An_{35}), and iron-rich pyroxene, but no alkali feldspar or aegirine are reported (Rogan et al., 1996). Differentiates in the Levering flow (CRB) contain plagioclase up to An_{25} and iron-rich augite (Hartley and Thordarson, 2009). The Hafnarhraun flow from Iceland contains mostly plagioclase, iron-rich augite, and glass, but little to no olivine (Nikkola et al., 2019). Because of fast quenching, the pillow lava differentiates discussed by Merle et al (2005) are glassy with microlites of plagioclase, clinopyroxene, and Fe–Ti oxides. Pigeonite is reported in differentiates from some HAT (Kuno, 1965; Goff, 1977, 1996) and in the Levering lava (Hartley and Thordarson, 2009). Both Kuno (1965) and Goff

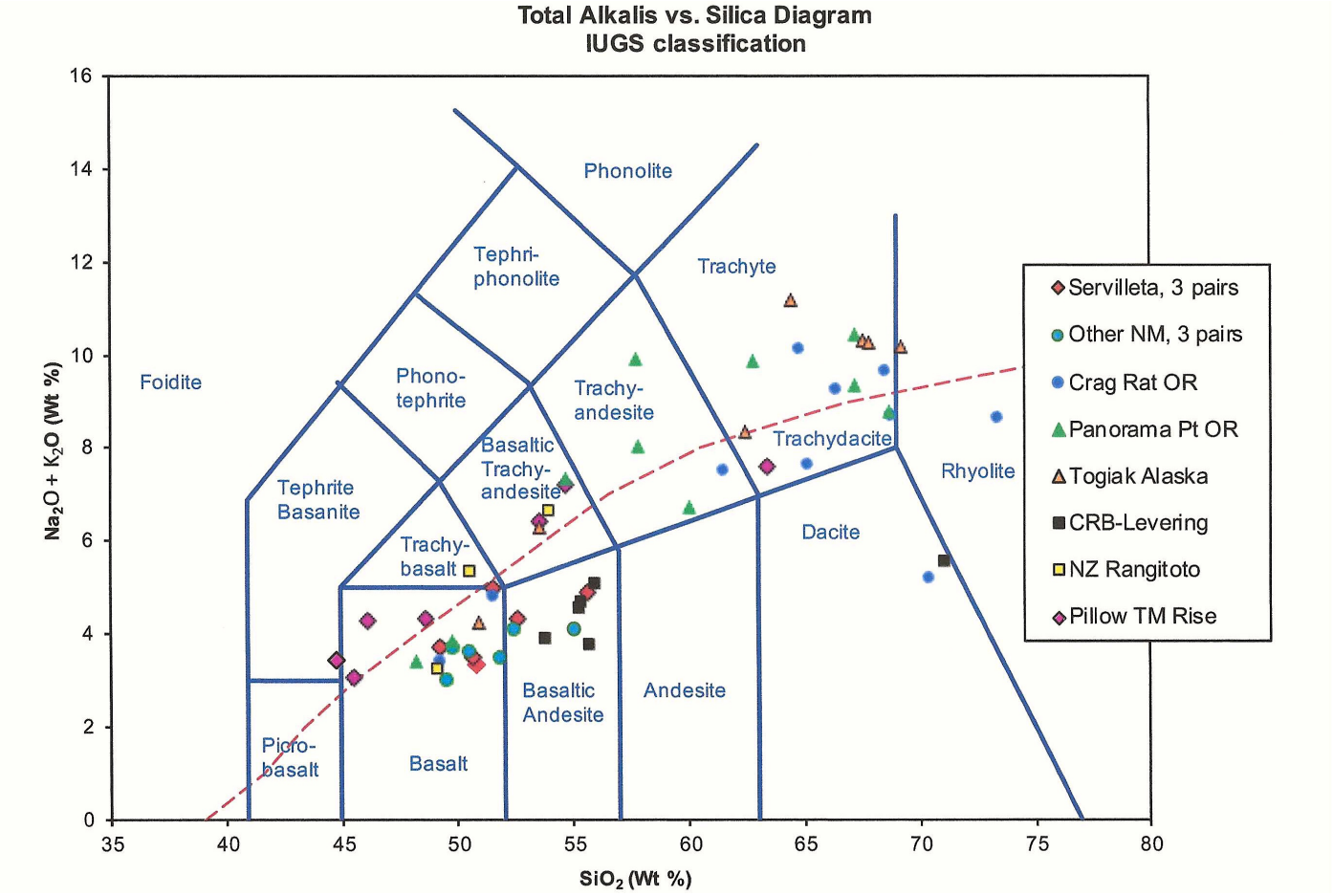


FIGURE 7. Plot of total alkali vs. silica for several basaltic locations hosting VC and associated VS; colors and symbols are different from those in Figure 5. Red dashed boundary separating alkalic from subalkalic (calc-alkaline) compositions is from Miyashiro (1978). Each mafic lava in key symbolizes the total of bulk rock host, VC and VS analyses, plus microprobe analyses of chilled bottom crust glasses and residual glasses in VC and VS (if available). Six host–VC/VS pairs from New Mexico show a "subalkalic" trend from basalt toward basaltic andesite, but no microprobe analyses of residual glasses have been reported to complete the trend. The Levering (CRB) trend from basaltic andesite to dacite is also subalkalic. Fractionation trends for other basaltic examples are distinctly alkalic during formation of VC, VS, and residual glasses, trending toward trachybasalt, trachyte, and even rhyolite (Crag Rat, Panorama Point, Togiak, Rangitoto, and the pillow basalt from TM Rise). Panorama Point and Togiak data were originally published in Goff (1977). Other data are discussed in text.

(1977, 1996) identified cristobalite/tridymite as vesicle linings in HAT. The cristobalite is of high-temperature vapor phase origin containing ≤4 wt% Al_2O_3 + Na_2O.

VESICLE CYLINDERS—THE GLOBAL PERSPECTIVE

Age, Tectonic Setting, and Bulk Chemistry of Host Lavas

VC with associated VS occur in basaltic rocks of Quaternary (e.g., Table 1) to Precambrian age (the Keweenaw flood basalts of Michigan, Fig. 3B and 3C; Cornwall, 1951). In New Mexico, identified VC-bearing flows are as old as Miocene (Table 1). VC-bearing lavas can occur in virtually any tectonic setting. They have been identified in volcanic and island arcs (e.g., Cascades, Japan, New Zealand), intracontinental rifts (e.g., RGR), volcanic intraplate lineaments (e.g., Jemez volcanic lineament), intraplate basaltic fields (e.g., Auckland, New Zealand), oceanic hot spot on a spreading center (e.g., Iceland), and flood basalt provinces (e.g., the CRB, Deccan Traps, and Keweenaw Basalt). They are also identified in pillow lavas dredged from the ocean floor. Thus, age and tectonic setting are not limiting factors in the development of VC. Rather, the primary cause is unusually high content of dissolved water in the source magma.

Lavas hosting VC and VS are often found in clusters of similar eruptions. For example, many VC-bearing flows are located in Quaternary basalts that straddle the Columbia River near Hood River, Oregon, and on the Modoc Plateau of California. Lavas of the Sentinel Bluffs and Wanapum Members of the CRB host many VC-bearing flows, and the Servilleta basalt in the Taos volcanic field contains several VC-bearing lavas.

Lavas containing VC and associated VS range in composition from borderline basanite to basaltic andesite (Fig. 5). Lavas described in this report range from about 44 wt% to 56 wt% SiO_2 and ≤5 wt% total alkalis (LOI free basis). Most documented examples of VC develop in OT or HAT basalts that have 2.0–4.5 wt% total alkalis. Previously, some examples were described as "alkali basalt" or "alkali olivine basalt" (e.g., Togiak basalt, Alaska), but on a TAS plot (Le Bas et al., 1986), these representatives are OT. To date, I have found no reported examples of VC in lavas of trachybasalt or basaltic trachyandesite composition. For example, the Mount Taylor composite volcano in New Mexico contains a multitude of trachybasalt to trachyandesite eruptions dated at 3.4–1.3 Ma (Goff et al., 2019, 2020), but no VC with associated VS have been recognized in their respective flows. Also, no recorded VC with VS have been identified in alkalic (trachybasalt) lavas with mantle xenoliths.

Continuity Within Flows

I previously stated that VC in smaller mafic eruptions occur throughout the entire flow (Goff, 1977, 1996), but this has not been adequately tested. As of now, it is not completely clear that VC preferentially develop near source, near terminus, or randomly. Further study of the AV, CV, and USB flows in New Mexico could provide more data on VC continuity and density because good exposures occur over broad areas in single and multiple flows. Complete continuity does not exist for many flood basalt lavas in the CRB. For example, the Museum flow, the highest member of the Sentinel Bluffs Member of the CRB (Reidel, 2005, p. 3), is a diktytaxitic flow containing VC and VS. It is well exposed along US Interstate 90 north of Vantage, Washington (Goff, 1996), and average VC spacing is about 20 cm (Costa et al., 2006, p. 299). However, the uppermost Sentinel Bluffs flows on Umtanum Ridge to the south, also diktytaxitic in texture, have no exposed VC (Goff, 1981, p. 17).

Time Frame of Development

Pure conductive cooling model

Because VC grow vertically, they develop in lavas that have virtually ceased movement. If the cooling history of the lavas and the temperature of formation of the VC are known, the length of time required for VC to grow can be estimated. Temperatures are determined from known eruptions and mineral equilibria, and viscosities are calculated from mineral compositions in both host and VC and/or VS to constrain conductive cooling models (e.g., Jaegar, 1961). An example for a 6-m-thick pahoehoe basalt flow erupted at 1150 °C and exposed to air on top was provided by Goff (1977, fig. 42; 1996, fig. 9). The VC begin growth at about 1075 °C, or about 1 day after the flow comes to rest, and pool into vesiculated pods and/or inject into VS 1–3 m below the flow top. For the chilled crust to become so rigid that differentiate cannot penetrate it requires temperatures approaching the solidus, about 1050 °C (Shaw, 1969; Helz, 1987). Using this value as a minimum temperature of ponding at the base of the chilled crust, VC will cease rising 2–3 days after the flow becomes stagnant. For a chilled crust 1.5 m thick, the VC rise 4.5 m in about 1.5 days, giving an average ascent rate of 3.5 x 10^{-3} cm/s.

Raising the temperatures of this example by 25 °C does not significantly change the calculation, but increasing the flow and/or crust thickness has greater impact. For a 12-m-thick flow, the mean ascent rate for first-formed VC is approximately doubled. For a 6-m-thick flow, no VC can grow after about 15 days because the interior of the flow will have cooled to near solidus temperature (see Goff, 1977, 1996, for details). For comparison, Caroff et al. (2000, fig. 9) calculate that VC would complete growth in a 5-m-thick flow in 3.5 days. Kuritani et al. (2010) determined that VC in the 6-m-thick Kutsugata flow (Japan) began growth about 1 day after the flow ceased movement and that formation of all "segregation products" (VC and VS) was complete after 20 days.

Cooling pahoehoe crust model

In a detailed paper on Kilauea pahoehoe sheet flows, an empirical equation was devised that estimated the time elapsed for a rigid crust to develop (Hon et al., 1994, p. 361). In the special case of VC-bearing flows, this would be the time at which VC cannot penetrate the bottom of chilled upper crust.

The equation is $t = 164.8\ C^2$, where t is the elapsed time in hours and C is the crustal thickness in meters. The flow lobe used to determine the equation was ≤2.5 m thick, and the temperature at the base of chilled crust was 1070 °C (see Hon et al., 1994, p. 161–162, for details). The thickness of chilled crust in "typical" VC-bearing flows is about 1.5 m (Goff, 1996, table 2); thus, the limiting time to grow VC would be 371 h, or 15 days, in remarkably good agreement with the pure conductive cooling model described above for a 6-m-thick flow. If the impenetrable crust is 2 m thick, the limiting time using the above equation would be 27 days. This equation does not depend on eruption temperature, viscosity, flow thickness, or other flow parameters. Basically, the thicker the flow crust, the longer the *implied* limiting time to grow VC, which does not make sense intuitively for "typical" flows.

Hartley and Thordarson (2009, p. 440) used the empirical equation above to calculate the emplacement time of VC in the Levering Basalt (CRB). In this case, the flow is ≤20 m thick and the crust is about 6 m thick. Because cooling to impenetrable conditions is dependent only on crust thickness, the limiting time on initial VC growth would be 247 days, or about 0.68 a. But the cooling history of the Levering flow is more complicated than a simple, relatively thin pahoehoe sheet flow as it exhibits multiple pulses of inflation (and thus probable crust development) and displays disrupted VC from earlier inflation events (Hartley and Thordarson, 2009, fig. 2b and p. 438).

Disrupted VC have also been documented in the Roza flow (CRB; Thordarson and Self, 1996, fig. 4), which commonly consists of two but can be up to five flow units of pahoehoe lava that has a complicated inflation and cooling history. The major flow units both have VC and VS; estimates of crust thickness vary, but for a crust thickness of 3.4 m in the upper flow unit, the limiting time for initial growth of VC, from the empirical equation above, would be 1,905 h, or 79 days.

These comparisons between the two cooling models indicate that more thought and calculations are required to determine the initial formation and growth times of VC and VS in thicker, more complicated pahoehoe flows with multiple injections of "pass through" lava. See discussion in Soderberg et al. (2024, p. 92) regarding growth and cooling of compound pahoehoe sheet flows.

VC Development and Growth

Vapor-differentiation versus gas filter pressing

Goff (1977, 1996) coined the term "vapor differentiation" for the process whereby residual liquids and water vapor are fractionated from host lava into bubble-rich vertical plumes (VC); this is the term most used by subsequent authors (e.g. Caroff et al., 2000; Merle et al., 2005). Anderson et al. (1984) proposed the term "gas filter pressing" (GFP) for the process during which "residual liquid migrates through a porous and permeable, but rigid, network of interlocking crystals in response to a pressure gradient generated by vapor-saturated crystallization." Their model was developed for segregation veins (i.e., VS) and segregation vesicles in one basalt and three basaltic andesites. Their four flows do not contain VC, although the groundmass of each flow has diktytaxitic texture. Therefore, the GFP model does not exactly apply to VC-bearing lavas.

The example basalt used by Anderson et al. (1984) is called Warner basalt, although in 1984 this name was applied to many HAT from the Modoc Plateau of the Cascades Range. It is interesting to compare calculated parameters used to generate the GFP model (Anderson et al., 1984, table 3) with those used by Goff (1977; 1996, table 2) for the Warner basalt at two locations where VC are present. The eruption temperature (T_e) used in the former study is 1265 °C, whereas in the latter T_e ranges from 1205 to 1235 °C. Calculated viscosity of the differentiate by GFP is 1×10^3 Pa-s, whereas in the latter calculated viscosity is 2.3×10^3 Pa-s. Anderson et al. (1984) studied a flow of Warner basalt only 1 m thick, whereas Goff (1977, 1996) studied Warner flows 7–8 m thick. Both studies used the empirical methods of Shaw (1972) to calculate viscosities from chemical analyses. As recapped by Goff (1996, p. 183), "vapor-differentiation and gas filter-pressing are terms with essentially identical meanings in the small-scale sense." The two terms are used interchangeably by most researchers (e.g., Caroff et al., 2000; Merle et al., 2005; Hartley and Thordarson, 2009, p. 441) but are confusingly applied by others (e.g., Nikkola et al., 2019).

Proposed growth mechanisms

Viewing horizontal cross-sections of basaltic rocks with high VC density (Fig. 2E; see also Goff, 1996, fig. 3a) reveals that VC grew upward as diapirs or plumes of low-density, relatively low-viscosity differentiate within the host lava. Goff (1977, p. 121–127) modeled VC growth as a Rayleigh–Taylor instability process using the equation of Selig (1965) for simple approximations (see also Plesset and Whipple, 1974). For application to a VC-bearing lava, the equation is dependent only on the thickness and viscosity of the host and the thickness and viscosity of a hypothetical bubble-rich layer that develops during vapor differentiation at the solidification front near the bottom of the flow (Fig. 8). This latter layer must be <10% the thickness of the host basalt (see also Costa et al., 2006). Using calculated viscosities from chemical analyses (Shaw, 1972) and field observations, Goff (1977, table 17) calculated preferred average spacings using the Selig equation (1965) that were in rough agreement with measured average spacings in four HAT lavas. Differences between calculated and measured spacings were +6%, +60%, −16%, and +8%. The apparent problem with this VC growth model is that the lower solidification front, and thus the lower bubble-rich layer, are ascending as the lava flow is cooling, and the lower layer is not preserved.

In an elegant set of experiments conducted by Costa et al. (2006, p. 299), diapirs of "segregated liquids" that grew by Rayleigh–Taylor instability were generated from very thin bubble-rich layers beneath much thicker layers of bubble-free liquids. The liquids used were golden syrup (diluted with water) and glycerin. Air bubbles were injected through a

porous sintered plate at the base of the experimental container (Costa et al., 2006, fig. 4). These researchers determined that the thickness of expelled vesicular melt required to produce VC spaced at ~20 cm was only 2 cm thick.

A different theoretical explanation for VC growth was proposed by Fowler et al. (2015), in which development of VC was compared to pipes that grow in solidifying binary alloys (sometimes called "freckles"). Although intriguing, the problem with this alternative is that no "bottom line" equation was offered that could combine field and calculated parameters to predict VC density or average VC spacing in observed basaltic lavas.

Dissolved Water in VC-Bearing Basaltic Magma

How much water is necessary?

VC develop in a wide range of water-rich basaltic lavas, but most researchers do not estimate a pre-eruption water content for these unique source magmas. However, according to Hartley and Thordarson (2009, p. 442), the Levering lava (CRB) contained only 0.3–0.4 wt% H_2O. Goff (1977, 1996) used an estimated water content of 0.5 wt% for viscosity and conductive cooling calculations in four HAT lavas. Experimental work by Beard and Lofgren (1992) indicated that HAT lavas contain ≥4 wt% H_2O. Sisson and Grove (1993) determined that HAT magmas contain between <1 wt% and >8 wt% H_2O depending on composition and physical conditions. Plank et al. (2013) indicated that most arc basalts have initial water contents of 2–6 wt%. Grove and Till (2015, table 1.1) show that subduction zone mantle melts contain ≤7.5 wt% H_2O. Obviously, the lower limit of water content required to develop VC and associated VS in basaltic magmas is not well constrained and needs further investigation, but apparently, most VC-bearing lavas, especially HAT, probably contained ≥0.5 wt% H_2O at eruption, some much more.

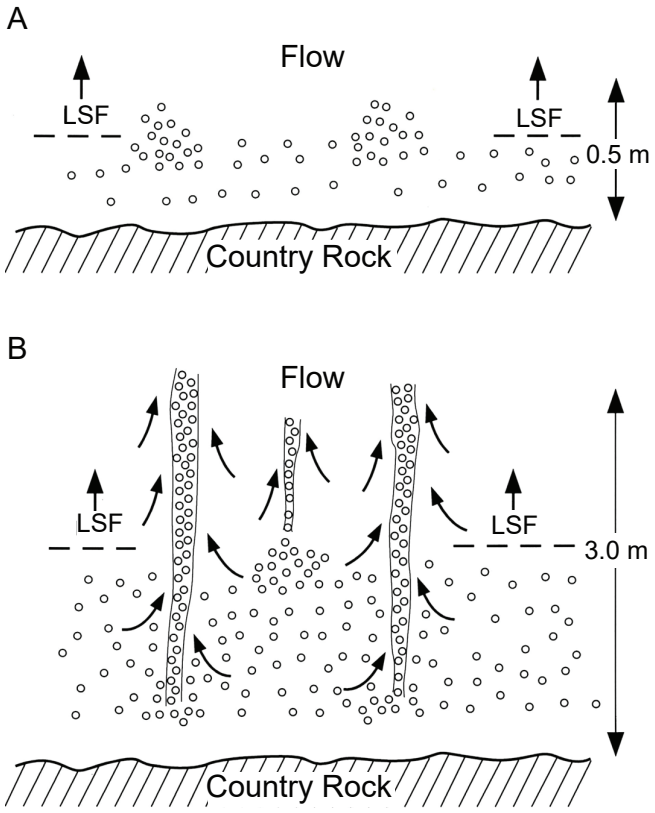


FIGURE 8. Cartoon depicting the formation of VC in lavas. A) Coalescing clusters of bubbles form proto-cylinders in the lower solidification front (LSF) near the base of the flow. B) Once a cluster of low-density bubble-rich lava begins to rise, residual melt and vapor in the diktytaxitic lava migrate into the low-pressure region created by this disturbance (gas filter pressing; Anderson et al., 1984). Continued accumulation of vapor and differentiate (i.e., vapor differentiation) and reduced overburden pressure from the enclosing lava cause the VC to increase in diameter as they rise toward the chilled upper crust. Upward migration of the solidification front causes new VC to begin growth at higher levels in the flow. Near-even spacing between VC is density controlled, possibly modeled by Rayleigh–Taylor instability (modified from Goff, 1996). Similar cartoons have been used by Costa et al. (2006, fig. 3) and Sheth et al. (2017, fig. 10) to model VC development and rise.

What is the origin of the water?

It is convenient to merely say that the excess water in VC-bearing basaltic lavas comes from "deep" sources. Most tholeiitic basalts are generated at depths of 50–75 km (Grove and Till, 2015). For HAT, so common in volcanic arc environments, many researchers have argued that the excess water comes from partial melting of the subducted slab or a combination of mantle peridotite and subducted material (Crawford et al., 1987; Bartels et al., 1991). For the RGR, Lipman (1969) indicated that tholeiitic basalts were sourced from higher levels in the mantle than alkali basalts. Baldridge (2004) states that basaltic melts beneath New Mexico are generated at depths of 50–75 km from an asthenospheric component that is variably contaminated by both lower and upper crustal materials including water. For flood basalts, the excess water must come from contamination of lower crust with mantle melts (Self et al., 2015, p. 449). But these studies do not explain the source of the excess water in VC-bearing basaltic magmas from the Icelandic hot spot on the Mid-Atlantic Ridge. Does this water originate entirely from the mantle?

Goff (1996, table 6) used bulk-rock oxygen isotopes in four host–VC pairs to determine if ^{18}O in HAT was of mantle or partial crustal origin. The results were inconclusive but suggested that the VC lavas had a small component of crustal ^{18}O. A more modern approach would be to analyze strontium, neodymium, lead, and osmium isotopes of the bulk rock and minerals from many VC and VS samples in the same cylinder or flow, or to determine water content from analyses of melt inclusions in olivine and plagioclase phenocrysts. A bottom-to-top strategy from host and VC pairs in two different tectonic environments, perhaps comparing HAT from Oregon to OT in Iceland, might also be successful.

Is a Trigger Necessary for VC Development?

All lava flows that contain VC have diktytaxitic texture, but the reverse is *not* true: Most flows with diktytaxitic texture do not develop VC. If VC growth is merely a matter of density

instability, most diktytaxitic flows should display VC. Perhaps VC growth is controlled by initial bubble size or by size restrictions in the initial rigid permeable framework of crystals (Costa et al., 2006). The mafic lavas that produce VC and associated VS exsolve copious amounts of water and other volatiles. Perhaps a "trigger" is required. This could be an earthquake or explosions at the vent area, which shake the ground and fresh nearby lava, similar to shaking a bottle of carbonated water. It is well known that earthquakes trigger volcanic eruptions and hydrothermal features (Legrand, 2022; Reed et al., 2024).

CONCLUSIONS

VC and associated VS in basaltic lavas are important to volcanologists, petrologists, and geochemists because they record natural differentiation and fractionation processes in single outcrops. VC with VS form only in pahoehoe lavas that have diktytaxitic texture attesting to a high volatile content, mostly dissolved water, in the source magma. VC and VS also provide excellent opportunities to determine and/or test contrasting temperature-dependent physical conditions (e.g., viscosity, density, porosity, cooling history, etc.) between host lava and resulting differentiates. A literature review shows that VC and VS develop in host lavas that are subalkaline to calc-alkaline, borderline basanite to basaltic andesite. VC with VS have not yet been documented in host lavas that are trachybasalt to basaltic trachyandesite in composition on conventional TAS diagrams. Mineralogically, host lavas are typically basaltic, but differentiates are exceptionally fractionated because they are concentrated in Fe–Ti oxides and contain fayalitic olivine, sodic plagioclase, alkali feldspar, occasional aegirine, rare amphibole and nepheline, trachytic–phonolitic–rhyolitic residual glass, and vapor-phase cristobalite/tridymite.

Most VC and associated VS are documented in host lavas 3–10 m thick (i.e., "typical flows"), but they are also found in flood basalts, pillow lavas, and very thin pahoehoe toes. VC grow from density instabilities resulting from the exsolution of large quantities of gas bubbles near the lower solidification front of static, cooling flows. The bubbles and residual liquids migrate through diktytaxitic groundmass pores of host lava to coalesce into near-vertical plumes or diapirs of frothy differentiate that rise into the still-molten core of the flow. This process is gas filter pressing caused by vapor differentiation and occurs before the network of crystals is too rigid to pass fractionated liquids. Rayleigh–Taylor instability is the model most commonly invoked to predict the rise of "evenly spaced" low-density plumes in water-rich basaltic lavas.

Important and interesting topics requiring additional investigation are (1) continuity of VC distribution and average closest spacing (VC density) throughout flows, (2) timing of VC growth in very thick, complicated flows (i.e., flood basalts), (3) minimum dissolved water content required to develop VC in host lavas, (4) source(s) of water from subducted slab, lower/upper crust, mantle, or combinations thereof, and (5) a possible "triggering" mechanism, given that most diktytaxitic, pahoehoe lavas do not grow VC. New Mexico has several identified VC-bearing lava locations that can resolve most of these research topics.

ACKNOWLEDGEMENTS

The pioneering work of Aaron C. Waters (University of California, Santa Cruz) and Hisashi Kuno (University of Tokyo) is gratefully appreciated. Valued assistance, dialogue, and correspondence were provided by Gerry Czamanske, Lou Calk, Brent Fabbi, Joe Hoare, Herb Shaw, Charlie Bacon, and Rosalind Helz (U.S. Geological Survey), A.T. Anderson (University of Chicago), Ian Smith (University of Auckland), Jamie Gardner, A.W. Laughlin, and Scott Baldridge (Los Alamos National Laboratory, LANL), Bill Rose (Michigan Technical University), M. Caroff (Université de Bretagne Occidental), R. Merle (Université de Nantes), Jim Stimac (consultant), and Nancy Riggs (University of Northern Arizona). The author thanks Dan Koning and Sean Connell (both New Mexico Institute of Mining and Technology) and Larry Crumpler (New Mexico Museum of Natural History) for encouraging the present effort. All costs for this manuscript, including analyses, were self-funded. Andi Kron (private contractor) prepared several of the figures. Cathy J. Goff (geologic consultant) completed a preliminary review of the draft manuscript. Jim Stimac and Larry Crumpler reviewed the final manuscript. Editorial handling was provided by Matt Zimmerer (New Mexico Bureau of Geology & Mineral Resources).

REFERENCES

American Geological Institute, 2005, Glossary of Geology: Alexandria, Virginia, American Geological Institute, 5th edition, 779 p.

Anderson, A.T., Swihart, G.H., Artioli, G., and Geiger, C.A., 1984, Segregation vesicles, gas filter-pressing, and igneous differentiation: Journal of Geology, v. 92, p. 55–72 (Table 3, analysis 143-M). https://doi.org/10.1086/628834

Aoki, K.-I., and Kudo, A.M., 1976, Major-element variations of Late Cenozoic basalts of New Mexico: New Mexico Geological Society, Special Publication 5, p. 82–88.

Arney, B., Goff, F., and Eddy, A.E., 1985, Chemical, petrographic, and K-Ar age data to accompany reconnaissance geologic strip map from Kingman to south of Bill Williams Mountain, Arizona: Los Alamos National Laboratory, Report LA-10409-HDR, 26 p.

Aubele, J.C., Crumpler, L.S., and Elston, W.E., 1988, Vesicle zonation and vertical structure of basalt flows: Journal of Volcanology and Geothermal Research, v. 35, p. 349–374. https://doi.org/10.1016/0377-0273(88)90028-5

Baldridge, W.S., 1979, Petrology and petrogenesis of Plio-Pleistocene basaltic rocks form the central Rio Grande rift, New Mexico, and their relation to rift structure, *in* Riecker, R.E., ed., Rio Grande Rift: Tectonics and Magmatism: Washington, D.C., American Geophysical Union, p. 323–353. https://doi.org/10.1029/SP014p0323

Baldridge, W.S., 2004, Pliocene-Quaternary volcanism in New Mexico and a model for genesis of magmas in continental extension, *in* The Geology of New Mexico, a Geologic History: New Mexico Geological Society, Special Publication 11, p. 313–330.

Bartels, K.S., Kinsler, R.J., and Grove, T.L., 1991, High-pressure phase relations of primitive high-alumina basalts from Medicine Lake volcano, northern California: Contributions to Mineralogy and Petrology, v. 108, p. 253–270. https://doi.org/10.1007/BF00285935

Beard, J.S., and Lofgren, G.E., 1992, An experiment-based model for the petrogenesis of high-alumina basalts: Science, v. 258, p. 112–115. https://doi.org/10.1126/science.258.5079.112

Bishop, D.T., 1969, Stratigraphy and distribution of basalt, Benewah County, Idaho: Idaho Bureau of Mines and Geology, Pamphlet 140, 22 p.

Carmichael, I.S.E., and Ghiorso, M.S., 1990, The effect of oxygen fugacity on the redox state of natural liquids and their crystallizing phases: Reviews in Mineralogy and Geochemistry, v. 24, p. 190–212. https://doi.org/10.1515/9781501508769-011

Caroff, M., Maury, R.C., Cotton, J., and Clement, J.-P., 2000, Segregation structures in vapor-differentiated basaltic flows: Bulletin of Volcanology, v. 62, p. 171–187. https://doi.org/10.1007/s004450000077

Cashman, K.V., Mangan, M.T., and Newman, S., 1994, Surface degassing and modifications of vesicle size distributions in active basalt flows: Journal of Volcanology and Geothermal Research, v. 61, p. 45–68. https://doi.org/10.1016/0377-0273(94)00015-8

Connell, S.D., 2008, Geologic map of the Albuquerque–Rio Rancho metropolitan area and vicinity, Bernalillo and Sandoval Counties, New Mexico: New Mexico Bureau of Geology and Mineral Resources, Geologic Map GM-78, 1:50,000. https://doi.org/10.58799/gm-78

Cornwall, H.R., 1951, Differentiation in lavas of the Keweenawan series and the origin of copper deposits of Michigan: Geological Society of America Bulletin, v. 62, p. 159–202. https://doi.org/10.1130/0016-7606(1951)62[159:DILOTK]2.0.CO;2

Costa, A., Blake, S., and Self, S., 2006, Segregation processes in vesiculating crystallizing magmas: Journal of Volcanology and Geothermal Research, v. 153, p. 287–300. https://doi.org/10.1016/j.jvolgeores.2005.12.006

Crawford, A.J., Falloon, T.J., and Eggins, S., 1987, The origin of island arc high-alumina basalts: Contributions to Mineralogy and Petrology, v. 97, p. 417–430. https://doi.org/10.1007/BF00372004

Dungan, M.A., Lindstrom, M.M., McMillan, N.J., Moorbath, S., Hoefs, J., and Haskin, L.A., 1986, Open system magmatic evolution of the Taos Plateau volcanic field, northern New Mexico: 1. The petrology and geochemistry of the Servilleta basalt: Journal of Geophysical Research, v. 91 (B6), p. 5999–6028. https://doi.org/10.1029/JB091iB06p05999

Dungan, M.A., Thompson, R.A., Stormer, J.S. and O'Neill, J.M., 1989, Excursion 18B: Rio Grande rift volcanism: Northeastern Jemez zone, New Mexico: New Mexico Bureau of Mines and Mineral Resources, Memoir 46, v. 1, p. 435–486.

Fowler, A.C., Rust, A.C., and Vynnycky, M., 2015, The formation of vesicular cylinders in pahoehoe lava flows: Geophysical and Astrophysical Fluid Dynamics, v. 108, p. 39–61. https://doi.org/10.1080/03091929.2014.955799

Fuller, R.E., 1931, The geomorphology and volcanic sequence of Steens Mountain in southeastern Oregon: American Journal of Science, 5th series, v. 21, p. 281–300. https://doi.org/10.2475/ajs.s5-21.124.281

Goff, F., 1977, Vesicle cylinders in vapor-differentiated basalt flows: Ph.D. thesis, University of California, Santa Cruz, 181 p. (A PDF can be obtained from F. Goff by email request).

Goff, F., 1981, Preliminary geology of eastern Umtanum Ridge, south-central Washington: Rockwell International, Rockwell Hanford Operations, Energy Systems Group, Report RHO-BWI-C-21, 94 p. with 1:24,000 geologic map. https://doi.org/10.2172/6670539

Goff, F., 1996, Vesicle cylinders in vapor-differentiated basalt flows: Journal of Volcanology and Geothermal Research, v. 71, p. 167–185. https://doi.org/10.1016/0377-0273(95)00073-9. (Downloadable PDF from journal offers only "blacked out" photos; contact F. Goff by email for corrected photos.)

Goff, F., and Kelley, S.A., 2020, Facts and hypotheses regarding the Miocene-Holocene Jemez Lineament, New Mexico, Arizona, and Colorado: New Mexico Geological Society, Special Publication 14, p. 1–15. https://doi.org/10.56577/FFC-71.101

Goff, F., Kelley, S.A., Goff, C.J., McCraw, D.J., Osburn, G.R., Lawrence, J.R., Drakos, P.G., and Skotnicki, S.J., 2019, Geologic map of the Mount Taylor Volcano area, New Mexico: New Mexico Bureau of Geology and Mineral Resources, Geologic Map 80, 1:36,000 scale map with 66-p. booklet. https://doi.org/10.58799/GM-80

Goff, F., McIntosh, W., Peters, L., Wolff, J.A., Kelley, S.A., Goff, C.J., and Osburn, G.R., 2020, Volcanic evolution of Mount Taylor stratovolcano, New Mexico: Facts and misconceptions: New Mexico Geological Society, Special Publication 14, p. 17–28. https://doi.org/10.56577/FFC-71.117

Gray, N.H., 1983, Mesozoic volcanism in north-central Connecticut: University of Connecticut, Department of Geology and Geophysics, unpublished field trip guide, p. 173–194.

Grove, T.L., and Till, C.B., 2015, Melting the Earth's upper mantle, in Sigurdsson, H., Houghton, B.F., McNutt, S.R., Rymer, H., and Stix, J., eds., The Encyclopedia of Volcanoes, 2nd edition: Amsterdam and Boston, Academic Press, p. 35–47. https://doi.org/10.1016/B978-0-12-385938-9.00001-8

Hartley, M.E., and Thordarson, T., 2009, Melt segregations in a Columbia River basalt lava flow: A possible mechanism for the formation of highly evolved mafic magmas: Lithos, v. 112, p. 434–446. https://doi.org/10.1016/j.lithos.2009.04.003

Helz, R.T., 1987, Differentiation behavior of Kilauea Iki lava lake, Hawaii: An overview of past and current work, in Mysen, B.O., Magmatic Processes: Physiochemical Principals: Geochemical Society, Special Publication 1, p. 241–258.

Hoare, J.M., and Coonrad, W.L., 1980, The Togiak Basalt, a new formation in southwestern Alaska: US Geological Survey Bulletin 1482-C, 11 p.

Hoffer, J.M., 1976, Geology of Potrillo basalt field, south-central New Mexico: New Mexico Bureau of Mines and Mineral Resources Circular 149, 31 p., 1 geologic map.

Hon, K., Kauahikaua, J., Delinger, R., and Mackay, K., 1994, Emplacement and inflation of pahoehoe sheet flows: Observations and measurements of active lava flows on Kilauea Volcano, Hawaii: Geological Society of America Bulletin, v. 106, p. 351–370. https://doi.org/10.1130/0016-7606(1994)106<0351:EAIOPS>2.3.CO;2

Jaeger, J.C., 1961, The cooling of irregularly shaped igneous bodies: American Journal of Science, v. 259, p. 721–734. https://doi.org/10.2475/ajs.259.10.721

KellerLynn, K., 2017, Petroglyph National Monument: Geologic resources inventory report: National Park Service Geologic Resources Division, Natural Resource Report NPS/NRSS/GRD/NRR—2017/1547, 57 p.

Kuno, H., 1960, High-alumina basalt: Journal of Petrology, v. 1, p. 121–145. https://doi.org/10.1093/petrology/1.1.121

Kuno, H., 1965, Fractionation trends of basalt magmas in lava flows: Journal of Petrology, v. 6, p. 302–321. https://doi.org/10.1093/petrology/6.2.302

Kuritani, T., Yoshida, T., Nagahashi, Y., 2010, Internal differentiation of Kutsugata lava flow from Rishiri Volcano, Japan: Processes and timescales of segregation structures' formation: Journal of Volcanology and Geothermal Research, v. 195, p. 57–68. https://doi.org/10.1016/j.jvolgeores.2010.06.003

Le Bas, M.J., Le Maitre, R.W., Streckeisen, A., and Zanettin, B., 1986, A chemical classification of volcanic rocks based on the total alkali–silica diagram: Journal of Petrology, v. 27, p. 745–750. https://doi.org/10.1093/petrology/27.3.745

Legrand, D., 2022, Which earthquake can trigger a volcanic eruption?: Journal of Volcanology and Geothermal Research, v. 432, 107698. https://doi.org/10.1016/j.jvolgeores.2022.107698

Lipman, P.W., 1969, Alkalic and tholeiitic basalt volcanism related to the Rio Grande depression, southern Colorado and northern New Mexico: Geological Society of America Bulletin, v. 80, p. 1343–1354. https://doi.org/10.1130/0016-7606(1969)80[1343:AATBVR]2.0.CO;2

Maldonado, F., Budahn, J.R., Peters, L., and Unruh, D.M., 2006, Geology, geochronology, and geochemistry of basaltic flows of the Cat Hills, Cat Mesa, Wind Mesa, Cerro Verde, and Mesita Negra, central New Mexico: Canadian Journal of Earth Science, v. 43, p. 1251–1268. https://doi.org/10.1139/e06-018

Merle, R., Caroff, M., Girardeau, J., Cotton, J., and Guivel, C., 2005, Segregation vesicles, cylinders and sheets in vapor-differentiated pillow lavas: Examples from the Torre-Madeira Rise and Chile Triple Junction: Journal of Volcanology and Geothermal Research, v. 142, p. 109–122. https://doi.org/10.1016/j.jvolgeores.2004.09.007

Miyashiro, A., 1978, Nature of alkalic volcanic rock series: Contributions to Mineralogy and Petrology, v. 66, p. 91–104. https://doi.org/10.1007/BF00376089

Nikkola, P., Thordarson, T., Ramo, O.T., and Heikkela, P., 2019, Formation of segregation structures in Hafnarhraun pahoehoe lobe, SW Iceland: a window into crystal-melt separation in basaltic magma: Bulletin of Volcanology, v. 81, 17 p. https://doi.org/10.1007/s00445-019-1330-9

O'Neill, J.M., 1989, Late Cenozoic volcanism, uplift, and erosion, Ocate volcanic field, north-central New Mexico, summary: New Mexico Bureau of Mines and Mineral Resources, Memoir 46, v. 1, p. 472–474.

Padovani, E.R., and Reid, M.R., 1989, Field guide to Kilbourne Hole maar, Dona Ana County, New Mexico: Mexico Bureau of Mines and Mineral Resources, Memoir 46, v. 1, p. 174–183.

Philpotts, A.R., and Lewis, C.L, 1987, Pipe-vesicles—An alternate model for their origin: Geology, v. 15, p. 971–974. https://doi.org/10.1130/0091-7613(1987)15<971:PVAMFT>2.0.CO;2

Plank, T., Kelley, K.A., Zimmer, M.M., Hauri, E.H., and Wallace, P.J., 2013, Why do mafic arc magmas contain ~4 wt% water on average? Earth and Planetary Science Letters, v. 364, p. 168–179. https://doi.org/10.1016/j.epsl.2012.11.044

Plesset, M.S., and Whipple, C.G., 1974, Viscous effects in Rayleigh-Taylor instability: Physics of Fluids, v. 17, p. 1–17. https://doi.org/10.1063/1.1694570

Reed, M.H., Barth, A., Taka'aki, T., Farrell, J., and Manga, M., 2024, A shake and a surge: Assessing the possibility of an earthquake-triggered eruption at Steamboat Geyser: Volcanica, p. 733–748. https://doi.org/10.31223/X58M37

Reidel, S.P., 2005, A lava flow without a source: The Cohassett flow and its compositional components, Sentinel Bluffs Member, Columbia River Basalt Group: Journal of Geology, v. 113, p. 1–21. https://doi.org/10.1086/425966

Rogan, W., Blake, S., and Smith, I., 1996, In situ chemical fractionation in thin basaltic lava flows: Examples from the Auckland volcanic field, New Zealand, and a general physical model: Journal of Volcanology and Geothermal Research, v. 74, p. 8–-99. https://doi.org/10.1016/S0377-0273(96)00059-5

Roland, S.K., and Walker, G.P.L, 1990, Pahoehoe and aa in Hawaii: Volumetric flow rate controls the lava structure: Bulletin of Volcanology, v. 52, p. 615–628. https://doi.org/10.1007/BF00301212

Rose, W.U., and Olson, J., 2013, Raspberry Island stop in Isle Royal: Keweenaw rift geology: Institute on Lake Superior Geology, Field Trip Guidebook, 59th annual meeting, Isle Royal, Michigan, May 25–30, 2013, 88 p. https://pages.mtu.edu/~raman/SilverI/IRKeweenawRift/Raspberry_I/Raspberry_I.html

Sakurai, R., Nakamura, M., Okumura, S., Mujin, M., and Nakatani, T., 2024, Vapor-phase crystallization from a hydrous silicate melt: An experimental simulation of diktytaxitic texture: Contributions to Mineralogy and Petrology, v. 179, 23 p. https://doi.org/10.1007/s00410-024-02105-4

Self, S., Coffin, M.F., Rampino, M.R., and Wolff, J.A., 2015, Large igneous provinces and flood basalt volcanism, in Sigurdsson, H., Houghton, B.F., McNutt, S.R., Rymer, H., and Stix, J., eds., The Encyclopedia of Volcanoes, 2nd edition: Amsterdam and Boston, Academic Press, p. 441–455. https://doi.org/10.1016/B978-0-12-385938-9.00024-9

Selig, F., 1965, A theoretical prediction of salt dome patterns: Geophysics, v. 20, p. 633–644. https://doi.org/10.1190/1.1439634

Shaw, H.R., 1969, Rheology of basalt in the melting range: Journal of Petrology, v. 10, p. 510–535. https://doi.org/10.1093/petrology/10.3.510

Shaw, H.R., 1972, Viscosities of magmatic silicate liquids: An empirical method of prediction: American Journal of Science, v. 272, p. 870–893. https://doi.org/10.2475/ajs.272.9.870

Sheth, H., 2020, "Pipe vesicles" in basalt: Trails of immiscible melt droplets sinking through a viscous basal thermal boundary layer: Earth-Science Reviews, v. 201, 103031. https://doi.org/10.1016/j.earscirev.2019.103031

Sheth, H., Patel, V., and Samant, H., 2017, Control of early-formed vesicle cylinders on upper crustal prismatic jointing in compound pahoehoe lavas of Elphanta Island, western Deccan Traps, India: Bulletin of Volcanology, v. 79, 12 p. https://doi.org/10.1007/s00445-017-1147-3

Sigmarrson, O., Thordarson, T., and Jakobsson, S.P., 2005, Segregation veins in Surtsey lavas, Iceland: Implications for volatile-melt induced magma differentiation: Geophysical Research Abstracts, v. 7, 10272. https://doi.org/10.1144/IAVCEl002.5

Sisson, T.W., and Grove, T.L., 1993, Temperatures and H_2O contents of low-MgO high-alumina basalts: Contributions to Mineralogy and Petrology, v. 113, p. 167–184. https://doi.org/10.1007/BF00283226

Smith, R.E., 1967, Segregation vesicles in basaltic lavas: American Journal of Science, v. 265, p. 696–713. https://doi.org/10.2475/ajs.265.8.696

Soderberg, E.R., Hart, R., Camp, V.E., Wolff, J.A., and Steiner, A., 2024, Stratigraphy, eruption, and evolution of the Columbia River Basalt Group, in McFaddan, M.D., and Pritchard, C.J, eds., Proterozoic Nuna to Pleistocene Megafloods: Sharing Geology of the Inland Northwest: Geological Society of America Field Guide 69, p. 81–121. https://doi.org/10.1130/2024.0069(05)

Thordarson, T., and Self, S., 1996, Sulfur, chlorine and fluorine degassing and atmospheric loading by the Roza eruption, Columbia River Basalt Group, Washington, USA: Journal of Volcanology and Geothermal Research, v. 74, p. 49–73. https://doi.org/10.1016/S0377-0273(96)00054-6

Thompson, R.A., Turner, K.J., Cosca, M.A., Chan, C.F., Morgan, L.E., Dungan, M.A., and Drenth, B.J., 2017, Day 2—The southern San Luis Basin and Taos Plateau volcanic field, in Field Trip Guide to Continental Arc to Rift Volcanism of the Southern Rocky Mountains—Southern Rocky Mountain, Taos Plateau, Jemez Mountains volcanic fields of southern Colorado and northern New Mexico: U.S. Geological Survey Scientific Investigations, Report 2017-5022-R, p. 29–70.

Thompson, R.A., Chan, C.F., Gilner, A.K., and Shroba, R.R., 2020, Geologic map of Petroglyph National Monument and vicinity, Bernalillo County, New Mexico: U.S. Geological Survey Scientific Investigations, Map 3447, scale 1:24,000. https://doi.org/10.3133/sim3447.

Wager, L.R., 1960, The major element variation of the layered series of the Skaergaard Intrusion and a re-estimation of the average composition of the hidden layered series and of the successive residual magmas: Journal of Petrology, v. 1, p. 364–398. https://doi.org/10.1093/petrology/1.3.364

Walker, F., 1956, The magnetic properties and differentiation of dolerite sills—A critical discussion: American Journal of Science, v. 254, p. 433–451. https://doi.org/10.2475/ajs.254.7.433

Waters, A.C., 1960, Determining direction of flow in basalts: American Journal of Science, Bradley Volume, v. 258-A, p. 350–366.

Wolfe, E.W., Ulrich, G.E., Holm, R.F., Moore R.B., and Newhall, C.G., 1987, Geologic map of the central part of the San Francisco volcanic field, north-central Arizona: U.S. Geological Survey, Open-file Map OF-1959 with 86-p. pamphlet.

Zimmerer, M.J., 2024, A temporal dissection of late Quaternary volcanism and related hazards within the Rio Grande rift and along the Jemez Lineament, USA: Geosphere, v. 20, p. 505–546. https://doi.org/10.1130/GES02576.1

Appendices can be found at
https://nmgs.nmt.edu/repository/index.cfml?rid=2026004



Western Tanager (*Piranga ludoviciana*) perched on limestone of Pennsylvanian Gray Mesa Formation, Sandia Mountains. Boulder of Sandia Formation pebbly sandstone in the background. Photograph courtesy of Celestyn Brożek.